Proceedings of the International Gas Turbine Congress 2003 Tokyo
November 2-7, 2003

IGTC2003Tokyo TS-020

The experience of CFD calculations for flow analysis in centrifugal compressor stages

Yuri B. Galerkin, Vladimir P. Mitrofanov and Alexei Y. Prokofiev

Compressor Department, TU Saint-Petersburg, Russia.
195251 Saint-Petersburg, Polytechnic street 29, Russia
Tel/Fax (812) 552 65 86,
e-mail: galerkin@mebil.stu.neva.ru

ABSTRACT

The problem of CFD calculations' validity still exists in respect of centrifugal stages. The vast information on flow structure, specific phenomena (measurements in rotating impellers are included) and performances of stages were used for comparison with CFD calculations by the codes TASCflow and FLUENT in cooperation with the Russian industry, the Universities of Germany and Poland. The results appeared to be sensitive to the applied turbulence models and exact numerical technology, but not the type of the code. In most cases the calculated performances are close to the measured ones. The certain flow peculiarities derived from calculations are not supported by results of direct measurements in the rotating impellers and flow visualization at the same time.

NOMENCLATURE

D_2 – impeller diameter
u_2 – impeller periphery speed
w – relative velocity
k – isentropic coefficient
Φ – flow rate coefficient
η – polytropic efficiency
b – blade's height
t – pitch
i – incidence angle
ω – angular velocity
ψ_i – head input coefficient
ψ_T – Euler head coefficient
ζ – loss coefficient

Subscripts

dif – diffuser
inl – inlet to an impeller
imp – impeller
tot – total parameters
des – design flow rate
exp – experiment
calc – calculation
0 – impeller inlet section
1 – blade channel inlet section
2 – impeller exit section
4 – diffuser exit section
0' – stage exit section

INTRODUCTION

The gas dynamic processes in centrifugal compressor stages has very complicated character due to high load of blades, small aspect ratio, U-turns in the meridian plane, effects of impellers' rotation. Detailed investigations in the TU SPb Compressor Department clarified many important gas dynamics phenomena. The physical and Math models were developed in result – so called Universal Modeling method – (Galerkin et al, 1995; Galerkin et al, 1999). The Universal Modeling codes are successfully and widely applied in design practice. It reduced an amount of necessary experiments and improved compressors' performances. More than 250 compressors of 39 types designed by Universal Modeling (about 4 million kWt of power in total) operate successfully in the pipeline industries of five countries, for instance.

The numerical analysis by statistically proven Universal Modeling can not give new, more deep information on a flow behavior. New step of progress is expected from the application of the modern CFD codes. Though still expensive and time – consuming, the CFD codes present detailed and complete information on the internal flow structure, behavior, and the overall performance of a stage and its elements as well.

Only one but vital problem arouses when CFD codes are applied to R&D practice. The turbulence models and wall functions used in the codes are derived from experiments and can not be universally valid therefore. Numerical character of calculations add some uncertainty to obtained results as well. The check of CFD results by experiments in (Galerkin et al, 2001) demonstrated that the problem of validity still exists in respect of centrifugal stages, as it existed in 1990–th related to all turbomachinery (Gallus, 1995). The calculations of centrifugal compressor stages must be proven by comparison with model test data before wide application for R&D.

The Compressor Department has vast information on flow specific phenomena, its structure and performances of stages. That data was used for comparison with CFD calculations. The calculations were executed in cooperation with Universities of Germany and Poland, Russian industry and independently by CD TU SPb. The codes TASCflow and FLUENT were applied to flow analysis in impellers, vaneless diffusers, return channels and complete stages. The influence of different turbulence models was investigated too.

EXPERIMENTAL DATA. FLOW BEHAVIOR IN IMPELLERS

All flow path elements are important to obtain good gas dynamic performances. The main attention to impellers in the present work is connected with important flow peculiarities that exist in impellers only and were thoroughly studied (by the Authors, in particular).

The experiments were executed at model test rigs (four rigs

Manuscript Received on March 28, 2003

with the same scheme and parameters -electrically driven, up to 600 kWt 0 - 18000 RPM). Model impeller diameters varied from 330 to 420 mm. Pressure traverse in control planes (sections) between stages' elements gives an information on a flow structure and performances of stages and its separate elements. The scheme of the centrifugal stage with control sections that divide its elements is presented at Fig. 1.

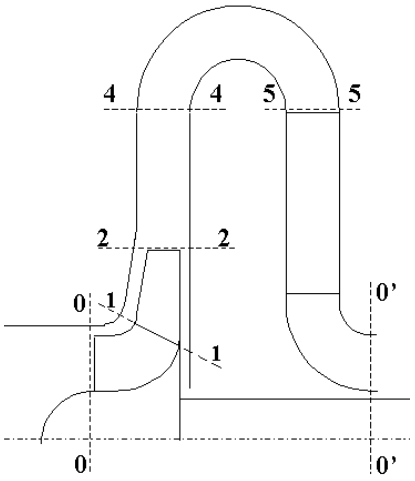

Fig. 1 Control sections in a centrifugal stage

The principles and technology of measurement inside rotating impellers by means of the especially designed pressure transducer were presented still in (Galerkin and Rekstin, 1969). Results of direct measurements were supported by flow visualization. It was executed by means of thin powder insertion to a flow path at a suction pipe. The powder followed flow stream lines well and sticks to channel surfaces in regions with low shear stresses as the proper similarity criteria were taken into account (Galerkin et al, 2000). The regions covered with powder correspond to low energy zones, i.e., to flow separation or wakes.

The measurements of static pressure on blades' surfaces are presented as so called "surface velocities". The proper total pressure was taken from the Bernoulli equation for relative co-ordinate system, inviscid flow. I.e., the supposition was made that the inviscid core exists in impeller channels. The measurements of total pressure inside impellers supported the validity of this supposition.

The comparison of the measured and calculated Q3D inviscid surface velocities at the blades of a typical 2D impeller are presented at Fig. 2.

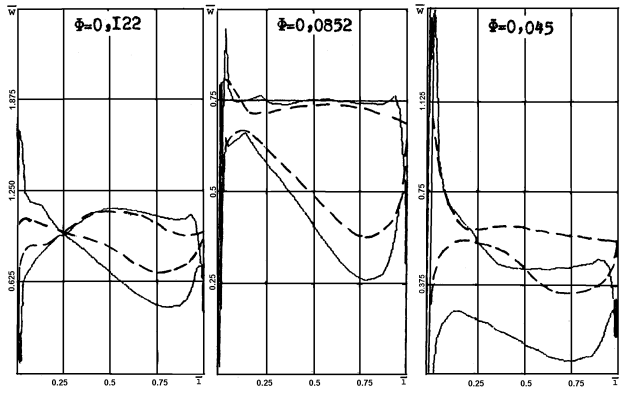

Fig. 2 Surface velocities at the mean blade-to-blade surface: $\Phi>\Phi_{des}$, $\Phi=\Phi_{des}$, $\Phi<\Phi_{des}$. Calculated Q3d inviscid – solid lines, measured – stroke lines – (Galerkin et al., 2000)

The total pressure coefficient diagrams at the exit of the same impeller (three blade – to – blade surfaces) are presented at Fig.3. There:

$$\tilde{P}^* = f(t/t_2) \quad \frac{\Delta\tilde{p}^*_{calc}}{\Delta\tilde{p}^*_{inviscid}}.$$

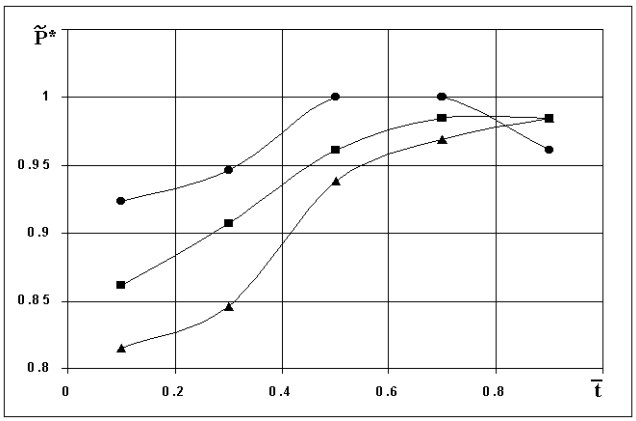

Fig. 3 Measured total pressure coefficients (relative) at the impeller 085/065 exit at three blade to-blade surfaces, $\Phi=0.065<\Phi_{des}$ – (Gerasimov, 1982). O - 20% from hub, □ - mean blade to blade surface, Δ - 20% from shroud

The data at Fig.2, 3 demonstrate:

1.The measured and calculated inviscid velocities are rather close by character and by value at the biggest part of impeller channels while incidence is close to zero or is negative ($\Phi \geq \Phi_{des}$). It demonstrates, that the viscid phenomena take place in the limited area of the channels only. The difference appears close to the exit at the suction side. The blades of the presented impeller was designed with the constant inviscid velocity along the suction side (no deceleration – no separation). The inviscid flow deceleration is inevitable in the region of the blades' unload at the exit. The real flow separates there – the measured velocity is constant up to the end of the channel while the inviscid flow decelerates. The limited wake area appears at the exit in result.

2. The real flow velocity diagrams lie higher than calculated inviscid while incidence is positive ($\Phi < \Phi_{des}$). Evidently, low energy viscid zones blockade the channels in this case. The traverse of the relative total pressures inside the channels (Gerasimov, 1982) demonstrates that the developed wake at the suction side appears and is responsible for the channel blockade. The results of flow visualization supports the above information – Fig.4.

3. The limited low shear stress zone takes place at the end of the suction sides while $\Phi \geq \Phi_{des}$. The constant velocity of the viscid flow there is characteristic to separation of flow or for wake (Fig.2). The vast zone of low stresses appears at the suction sides while $\Phi < \Phi_{des}$ (Fig.4). The zone starts from the leading edge near the shroud but the flow separates at the middle of the blade at the hub only. I.e. the zone is of 3D character. The earlier separation at the shroud is the result of higher velocities and stronger deceleration there. The meridian velocities at different blade – to – blade surfaces at Fig.5 (Q3D invscid calculations) demonstrates it.

4. The wake at the suction side is the only place of developed low energy zones in the impeller at any practically important flow rate. The information above is supported by data on two dozen of different impellers tested by the same way.

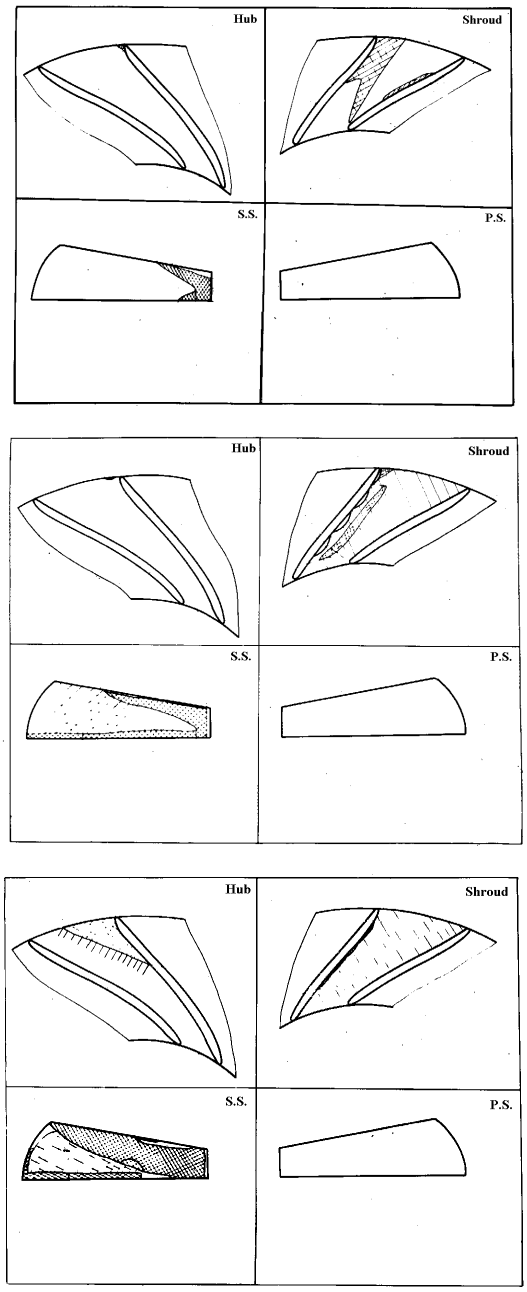

Fig. 4 "Powder" flow visualization at the impeller 085/065 – (Galerkin et al., 2000)

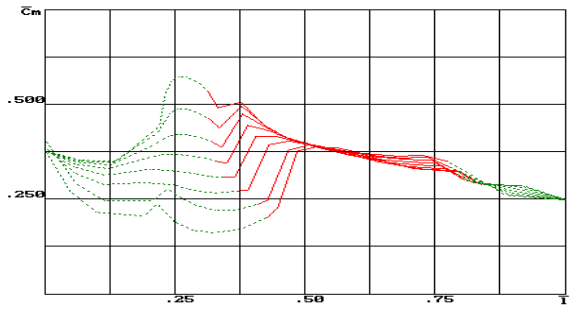

Fig. 5 Meridian velocities at the seven blade-to-blade surfaces. Q3D inviscid calculations, impeller 085/065. Red color – velocities inside blade channels (sections 1 – 2)

The absence of any noticeable separation at the pressure side of blades can be easily explained by the action of normal inertia forces. The appearance of a separation or wake at the pressure side would lead to increase of flow deflection to the direction of u_2, that means increase of work input by increase pressure difference at the blades. The flow in a zone of separation has insignificant kinetic energy. It could not create additional pressure that is necessary for increase of the blade's load. The normal inertia forces simply suppress any attempt of the flow to separate from the pressure side of blades. The only separation effects at blades' pressure sides are registered by detailed measurements by microprobes (Galerkin et al., 2000) near the leading edge while incidence angle $i << 0$ and the blade load is negative there.

The suppression of separation effects at the pressure sides of blades can be explained by detailed analysis of boundary layers' behavior as well (Johnston, 1970). The normal turbulence component is activated by normal inertia forces at pressure sides ("flow destabilization") and the boundary layer stays thin independent of the velocity gradient along the surface. The secondary flows at discs transport low energy particles away from the pressure side of blades. It is one more reason why any significant flow separation does not occur there. To the contrary, easy wake formation takes place while velocity decelerates along the suction side of blades. The mentioned above effects influences flow behavior in opposite directions in comparison with pressure sides of blades. The wake formation starts at comparatively small deceleration there.

As it is clear from meridian velocities' diagram at Fig. 5, the significant flow deceleration takes place along the concave surface of the curve-linear axis-symmetric channel between sections 0 – 1. The expected flow separation never been registered there in accordance with flow visualization results. The wind tunnel tests of the channels imitating the meridian shape of the inlet U-turn channel + impeller are presented in (Galerkin et al., 2000). The tests demonstrated absence of any separation at the concave surface between sections 0 – 1, despite sufficient flow deceleration along it. The normal inertia forces suppress formation of low energy zone there by the same way as at the pressure sides of blades.

The mentioned wind tunnel tests has shown the intensive separation at the shroud surface of the model channel. The meridian velocity deceleration is responsible for it. To the contrary, visualization and direct measurements in real impellers has never shown this phenomena (the separation never occurs at hubs as well). This contradiction can be explained by influence of secondary flow on the shroud and hub surfaces. The flow particles are subjects of Coriolis force in the rotating impellers. This force is rectangular to flow direction. As the secondary flow is rectangular to the flow in the core, the Coriolis acceleration $a_{cw_{sec}} = 2\omega w_{sec}$ produced by the secondary flow is directed along the core flow. The proper impulse adds momentum to the gas particles on the shroud and hub surfaces. The boundary layer profiles remain full and shear stresses are high enough to prevent separation.

COMPARISON OF EXPERIMENTAL AND CALCULATED PERFORMANCES

The stage type K101-1consisted of 2D impeller + vaneless diffuser + return channel was tested at the Compressor Department at M_u= 0.6 – 0.9. Total and static pressures were measured in control planes between stage's elements. The proper performances were calculated in the SPA "AVIADVIGATEL" (Perm city, Russia) by the licensed code TASCflow (k-ε turbulence model, blind test). The disk friction and leakage losses in the impeller's labyrinths were not modeled. These losses were eliminated from the experimental data by calculations with well-proven semi-empirical equations. The obtained results are presented at Fig. 6, 7 (stage's normalized parameters are evident from performance curves).

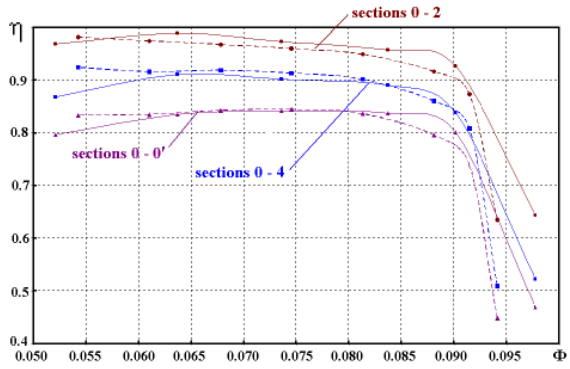

Fig. 6 Stage K101-1 efficiency comparison (M_u=0.6). Solid lines – experiment, dashes – calculation.

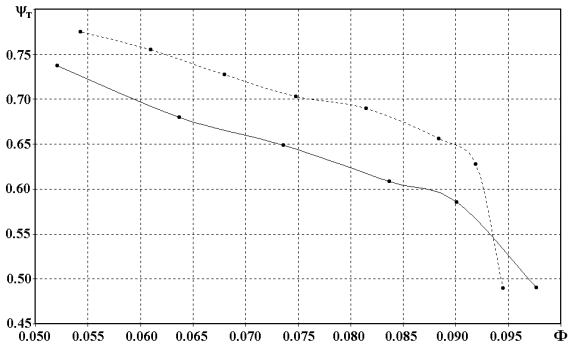

Fig. 7 Stage K101-1 work input coefficient comparison (M_u=0.6). Solid line – experiment, dashes – calculation

The efficiency prediction in all three control planes (after the impeller, after the diffused and of the whole stage) at Fig.6 seems to be good in the bigger part of the performance range. The calculation overestimates losses at big negative incidences ($\Phi > \Phi_{des}$) and underestimates at big positive incidence ($\Phi < \Phi_{des}$) though. The prediction of the work coefficient (Fig.7) is less impressive. The calculated $\psi_T = c_{u2} / u_2$ exceed the measured one at about 10% in the practically important part of the performance range. It means also, that the loss prediction is not very accurate, though the efficiency prediction is very good. It is known, that efficiency, work coefficient and loss coefficient are connected by the next equation:

$$\eta_{imp} = 1 - \frac{\zeta_{imp}(w_1 / u_2)^2}{2\psi_T}.$$

In the above case the measured and calculated efficiencies are very close, while calculated work coefficient is about 10% bigger. It means, that the calculated losses are bigger than the measured on the same percentage.

The measured and calculated (TASCflow, 470000 elements) performances were compared for the another stage (type 085/065) in control planes after 2D impeller and after vanelesss diffuser at M_u=0.60, 0.79 (k-ε model), and 0.871 (k-ε RNG model) (Galerkin et al., 2001). The applied code reacted well on Mach number variation. The work coefficient modeling was more satisfactory in this case – the calculated value was only 5% bigger at the design flow rate, while at the surge limit the calculated and measured values were equal. The efficiency of the 2D impeller + vaneless diffuser was predicted very well in vicinity of the design point (it means at the same time, that calculated losses were 5% bigger than the measured ones). The comparison of loss coefficients of the impeller (between sections 0-0/2-2) and the vaneless diffuser (between sections 2-2/4-4) is presented at Fig. 8. The calculated losses are bigger in the impeller and vice versa in the diffuser, being similar (experimental and calculated) in character.

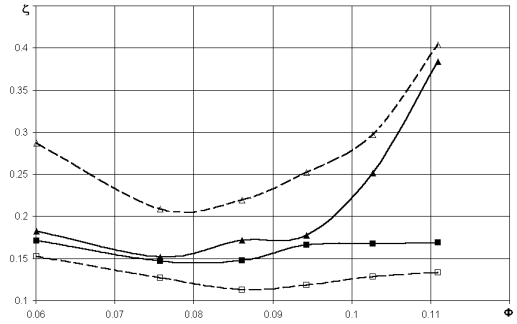

Fig. 8 Measured and calculated loss coefficients of the 2D impeller and the vaneless diffuser, M_u=0.6 – stage type 085/065 (Galerkin et al, 2001). Solid lines – experiment, dashes – calculation. Δ - sections 0 - 2, □ - sections 2 - 4

The same stage type 085/065 was the object of the numerical calculations by the code FLUENT with the results presented at the (Puzyrewski et al, 2001, Flaszynski et al, 2002). Different turbulence models were applied. The data for one flow rate regime are presented at the Table below. The calculated values that differ less than 0.5% from measured are presented by bold figures.

TABLE. Experimental and calculated data on the stage 085/065, M_u=0.60 (Puzyrewski et al, 2001; Flaszynski et al, 2002) Flow rate coefficient Φ=0.0952 (Φ_{des} =0.0852)

Parameter / Model	$\eta^*_{0\text{-}2}$	$\eta^*_{0\text{-}4}$	$\Delta\eta^*_{2\text{-}4\ calc}$/ /$\Delta\eta^*_{2\text{-}4\ exp}$	ψ_T / ψ_{Texp}
Exp	0.945	0.892	1.0	1.0
k–ε standard	0.906	**0.891**	1.046	1.046
k–ε realisable	0.928	0.910	1.018	1.018
k–ε RNG	**0.942**	0.920	0.415	**0.995**
k–ε RNG DVM	**0.938**	0.915	0.434	**0.998**
Low Re k–ε	0.921	0.904	0.321	1.026

Some remarks on the Table's content:

- Models κ–ε RNG and κ–ε RNG DVM are most precise in the impeller efficiency and work coefficient prediction.
- Model κ–ε is most precise in the impeller + diffuser efficiency prediction.
- All models underestimate losses in the vanelesss diffuser. The calculated values are in the range 32 – 43% of the measured.

Continuing the discussion let us remind that experimental data on total pressure measurements in the section 2-2 couldn't be treated as quite reliable. The reason is that usual pressure probes register unsteady jet-wake flow in this section. The correlation between real flow energy and an arbitrary time-averaged measured total pressure is uncertain. It is assumed that that measurements at the exit of a vaneless diffusers are more reliable, as a mixing process is practically finished before the section 4-4. The κ–ε standard model gives quite good correlation in the section 4-4. Here we again return to the situation, while good prediction of efficiency and bigger calculated work coefficient mean higher level of calculated losses. The performance of the stage, that was computed by the κ–ε RNG model appeared to be non-satisfactory left of the design point – the calculated losses were far too big.

The comparatively low flow rate stage type 028 was the object of the numerical analysis executed in the Center of High-speed Cluster Computational Technology of the TU SPb headed by Dr.-Ing. hab., Prof. N.Shabrov. The code FLUENT (κ–ε standard model) was applied. The comparison is presented at Fig. 9. The

calculated work coefficient is less than the measured one (4.2%) at the design flow rate – contrary to the cases above. Measured and calculated values are equal at the surge flow rate. Calculated efficiencies of the impeller (sections 0 - 2) and the impeller + vaneless diffuser (sections 2 - 4) are very close in character but differ in values too much. The data in the table below show that calculated losses in the impeller and in the vaneless diffuser smaller than the calculated ones twice or more - depend on the flow rate.

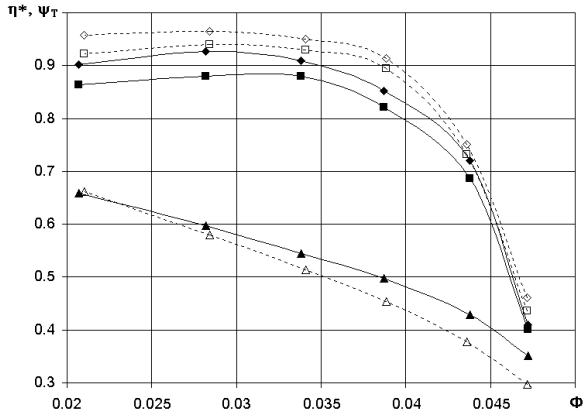

Fig. 9 Stage 028 efficiency and work input coefficient comparison (M_u=0.6). Solid lines – experiment, dashes – calculation. ◊ - efficiency of the impeller (sections 0 - 2), □ - efficiency of the impeller + vaneless diffuser (sections 0 - 4), Δ - work input coefficient

TABLE. Comparison of calculated and experimental data on the stage type 028, M_u=0.60

Φ	$\Delta\eta^*_{0\text{-}2\ calc}/\Delta\eta^*_{0\text{-}2\ exp}$	$(\Delta\eta^*_{2\text{-}4\ calc})/(\Delta\eta^*_{2\text{-}4\ exp})$	$\psi_{T\ calc}/\psi_{Texp}$
0.0472	0.913	2.691	0.845
0.0438	0.890	0.557	0.880
0.0387	0.588	0.602	0.914
0.0338	0.544	0.736	0.942
0.0282	0.487	0.537	0.971
0.0207	0.435	0.913	1.006

Contrary to the impeller and diffuser, the calculated losses are bigger in the return channel (Fig.10). The design point corresponds to $i_5 = 7^0$, where calculations gave 12% higher losses.

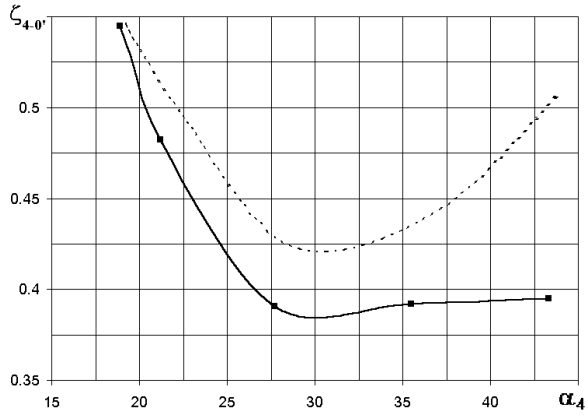

Fig. 10 Measured and calculated loss coefficients of the return channel, M_u=0.6 – stage type 028. Solid lines – experiment, dashes – calculation

The numerical flow visualization in the impeller 028 demonstrated that wakes were insignificant at the suction sides of blades at the design and lower flow rates. This hardly realistic result was may be the consequence of comparatively little number of elements in the blade channel (220000).

SURFACE VELOCITY DIAGRAMS' COMPARISON

Pressure distribution along the impeller 085/065 blades was measured on the middle blade to blade surface at different flow rates (M_u = 0.6). The results are presented as so called surface velocities (Seleznev and Galerkin, 1982). The equation below is obtained in a supposition that an inviscid core exists inside an impeller:

$$w/u_2 = (M_u^2 (D/D_2)^2 - (2/(k-1)) ((p/p_{inl\ tot})^{(k-1)/k} - 1))^{0.5} / M_u,$$

where D - a diameter where a measuring point is located at a blade.

It was shown in the (Galerkin et al, 2001) that the TASCflow calculated velocity diagrams differ from the measured ones the bigger the bigger flow rate is. The same result was obtained for the same object while the code FLUENT was applied (Puzyrewski et al, 2001; Flaszynski et al, 2002) – Fig.11. It is important to remind (Fig.2), that the calculated inviscid quasi-3D diagrams are very close to the measured ones at $\Phi >> \Phi_{des}$. The last means that viscid effects are of small significance at the regimes of high flow rates in reality. The same is demonstrated by flow visualization at Fig.4. Evidently, the reason of the poor correlation of the calculated TASCflow and FLUENT velocity diagrams with experiments is the result of overestimation of the viscid effects while $\Phi >> \Phi_{des}$.

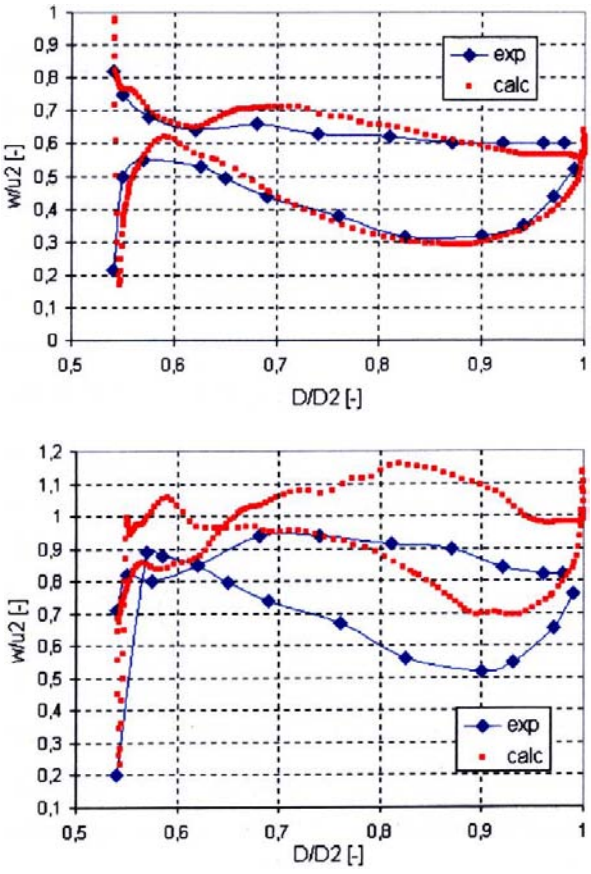

Fig. 11 Calculated and measured surface velocities in the impeller 085/065 – (Puzyrewski et al, 2001; Flaszynski et al, 2002). Above $\Phi = 0.0683 < \Phi_{des}$, below $\Phi = 0.11 > \Phi_{des}$

PHYSICAL EFFECTS IN THE FLOW PATH

Numerical visualization in many cases gives results that seems to be quite close to reality. Fig.12 demonstrates zones of the shear stresses on the shroud surface of the return channel of the stage type 028, while the incidence angle is positive. Low shear stresses' zones (are dark on the figure) correspond to flow separation. The physical "powder" visualization gave similar result.

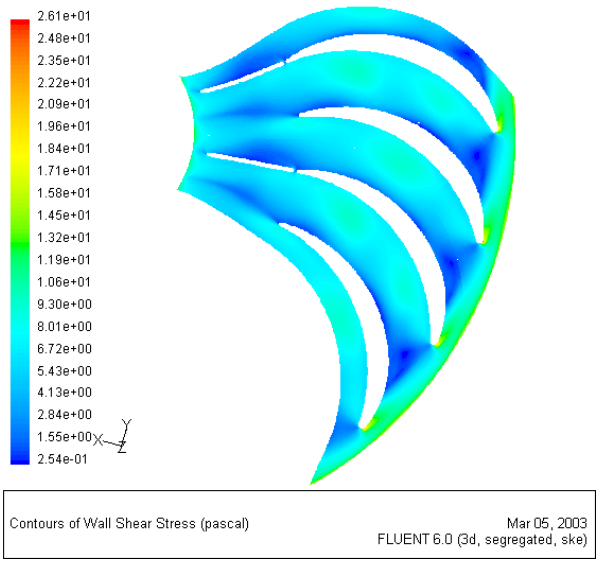

Fig. 12 Low shear stress zones at the hub surface of the return channel. Stage type 028, incidence $i_5=13^0$

The numerical flow visualization at $\Phi \le \Phi_{des}$ gives usually good results usually as well (the impeller 028 was an exception). The calculated velocity vectors near the suction surface at $\Phi < \Phi_{des}$ are presented at Fig.13 (Puzyrewski et al, 2001; Flaszynski et al, 2002). The picture is very typical in accordance with the physical visualization data and with results of direct measurements inside impellers.

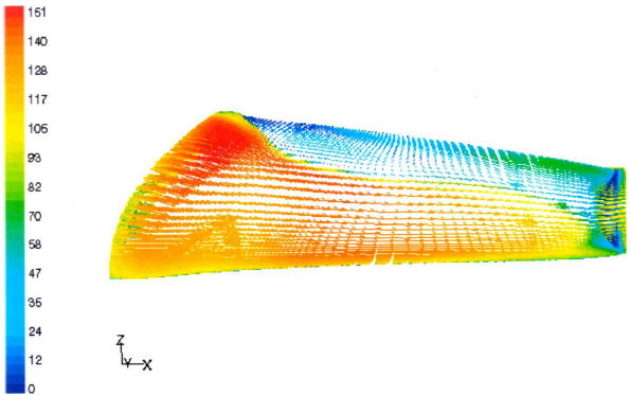

Fig. 13 Calculated velocity vectors 3 mm above the blade's suction side. Impeller 085/065, $\Phi = 0.0683 < \Phi_{des}$ (Puzyrewski et al, 2001; Flaszynski et al, 2002)

Unfortunately, in all analyzed cases the numerical visualization in impellers demonstrated effects that are exaggerated or absent completely in reality. The mentioned above mismatching of velocity diagrams for the impeller type 085/065 calculated both by TASCflow and by FLUENT is connected with the separation effects on the shroud. The Fig. 14 and 15 show separation zones that were not detected experimentally:

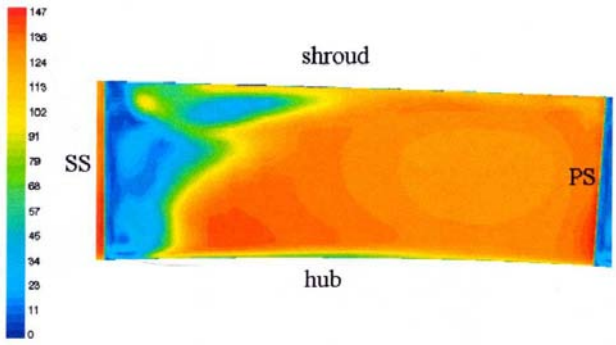

Fig. 14 Velocity contours as seen along a radius at the impeller exit (shroud is above, blade suction side is on the left). Off design regime $\Phi = 0.0952 > \Phi_{des}$, $M_u = 0.6$. The impeller 085/065, calculation by FLUENT (Puzyrewski et al, 2001; Flaszynski et al, 2002)

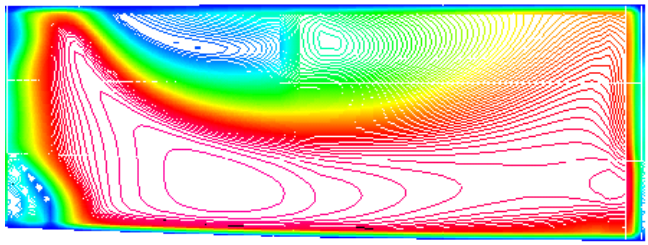

Fig. 15 Velocity contours as seen along a radius at the impeller exit (shroud is above, blade suction side is on the left). Off design regime $\Phi = 0.122 > \Phi_{des}$, $M_u = 0.6$. The impeller 085/065, calculation by TASCflow (Galerkin et al, 2001)

One more typical mismatch is demonstrated at Fig.16. The calculations by the FLUENT (Puzyrewski et al, 2001; Flaszynski et al, 2002) detected flow reverse zone at the hub surface in the curve - linear axis – symmetric channel before the blades. The separation were detected numerically at all flow rates. In result, the calculated meridian velocities near the hub before the leading edge are very low and independent of the flow rate – Fig.17.

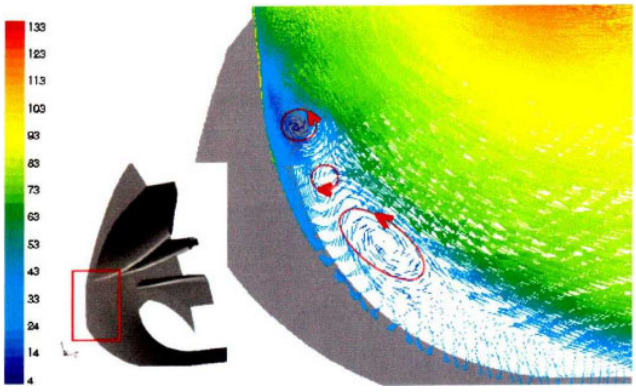

Fig. 16 Return flow at the hub surface in the axis symmetric channel before blades. Impeller 085/065, FLUENT, κ –ε RNG turbulence model, FLUENT (Puzyrewski et al, 2001; Flaszynski et al, 2002)

As it was mentioned, the "powder" visualization has not detected this phenomena. The impeller 085/065 was also tested at the special "water" test rig, where the working media left traces at the film of the fresh oil paint covering the impeller surfaces (Gerasimov, 1982). The photo at Fig. 18 shows the flow traces on the hub surface inside the blade channels and before them – i.e., in

the axis – symmetric channel before blades No reverse flow is visible in the object under discussion.

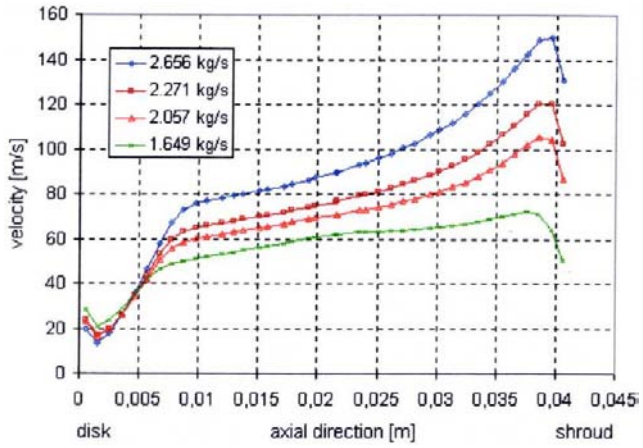

Fig. 17 Relative velocities along the leading edge of blades at different flow rates (Puzyrewski et al, 2001; Flaszynski et al, 2002)

One more consideration is connected with the results of the direct measurements. The surface velocities were defined in the impeller 085/065 at the number of blade – to - blade surfaces. The closest to the hub one was located at 3% of the inlet blade height. In accordance with data at Fig 16 the velocity at the blade's inlet is constant and independent of the flow rate. The low velocity level must correspond to big incidence angle there independent of flow rates. The data at Fig 19 (Gerasimov, 1982) show that direct measurements do not support it. The measured surface velocity diagrams at this blade – to – blade surface react on the flow rate quite as usual – the small flow rate corresponds to positive incidence, while big flow rate leads to the negative incidence.

Fig. 18 Flow traces at the hub surface of the impeller 085/065, $\Phi_{des} = 0.085$. "Water" test rig visualization (Gerasimov, 1982)

The visualization of the same impeller by the TASCflow code is presented at Fig. 20. The reverse flow is not detected by this calculation (the result is published by courtesy of Dipl. – Ing A.Toews, Dortmund, Germany).

CONCLUSION

The Compressor Department of the TU Saint-Petersburg has at its disposal big amount of information about performances and flow behavior in centrifugal compressor stages. The results of direct measurements of flow in rotating impellers and its visualization are especially important to check validity of the modern numerical codes. The presented above data of calculations could not pretend to be the universal answer to the validity problem due to limited amount of calculations. Undoubtedly, the modern Navier-Stokes codes are powerful instruments for researchers and engineers. Rather good prediction of overall performances in most cases and performances of stator elements are promising. Some predicted details of flow behavior in impellers were not in good correspondence with physical experiments, though. Some improvements on a base of numerical simulations could not be effective therefore. The problem deserves more attention and efforts.

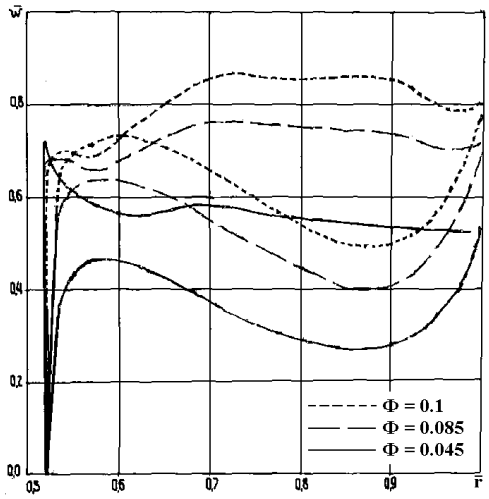

Fig. 19 Impeller 085/065. Measured surface velocities at the blade-to-blade surface 3% above hub. Three different flow rates (Gerasimov, 1982)

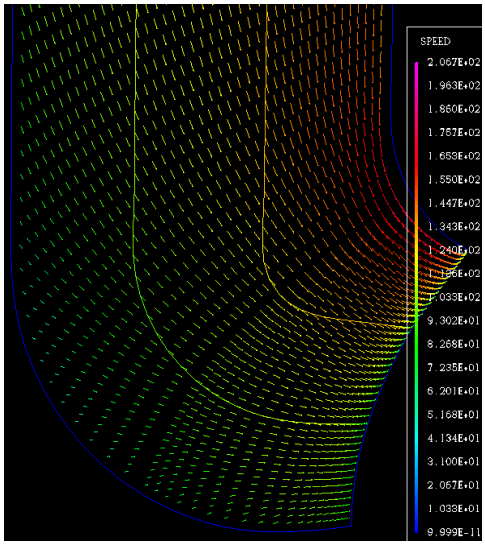

Fig. 20 Velocity vectors at the hub surface in the axis symetric channel before blades. Impeller 085/065, FLUENT, κ–ε turbulence model, TASCflow

REFERENCES

Galerkin Y.B. and Rekstin F.S., Test methods for centrifugal compressors . Mashinostroenie, 1969, 303 p.

I.Galerkin, K.Danilov, E.Popova. Universal Modelling for Centrifugal Compressor Optimal Design. VDI Berichte, N 1208, Hannover, 1995.

Y. Galerkin, K.Danilov and E.Popova. Design philosophy for industrial centrifugal compressors, IMechE Conference transactions “Compressors and their systems”, London, 1999.

Y.Galerkin et al. Transactions of the compressor’s scientific school in the TU Saint-Petersburg. NPC SPb TU, 2001, 443 p. (in Russian).

Y. Galerkin, V. Mitrofanov, M.Geller and F. Toews. Experimental and numerical investigation of flow in industrial centrifugal impeller. – Inernational Conference on Compressors and their Systems. 2001, London: City University, UK. p. 251-259.

Gallus H.E. Recent Research Work on Turbomachinery Flow. Yokohama International Gas Turbine Congress, Yokohama, 1995.

Gerasimov A.V., Flow structure and head losses in the centrifugal impellers, designed by the LPI method. Ph.D. thesis, Leningrad Polytechnic Institute, 1982 (in Russian).

Johnston J.P. “The Effects of Rotation on Boundary Layer in Turbomachine Rotors”. Report MD-24, Mech. Engrg. Stanford University, 1970, to be published in NASA SP304.

P. Flaszynski, Yu. B. Galerkin and R. Puzyrewski. "Experimental and numerical identification of separation zones ion the centrifugal compresor" Proceedings of International Conference SYMKOM 2002 Compressor& Turbine Stage Flow Path Theory. Experiment & User verification. Poland, Lodz, 23-25 October 2002, pp. 47-54.

R. Puzyrewski, Yu. B. Galerkin and P. Flaszynski. "Direct and inverse numerical calculation for the tested centrifugal impeller" Proceeedings of XI. Internationale Tagung Forschung Praxis und Didaktik im Modernen Maschinenbau. Germany, Stralsund, den 17-19 Oktober 2001, pp.41-48.

Seleznev K.P., and Galerkin Y.B., 1982, "Centrifugal Compressors". Maschinostoenie, 1982. Leningrad, 271 p.(In Russian).